Electronic Supplementary Information

A chiral coordination polymer with double coaxially nested helical chains exhibiting spin-canting antiferromagnetism

Hui-Jie Lun[a], Sa-Sa Cui[a], Hai-Jiao Li[a], Qi Ping[a], Hao-Han Song[a], Ya-Min Li*[,a], Yu Ru[a], Yan-Long Bai[a] and Sheng-Chang Xiang*[,b]

[a] *Henan Key Laboratory of Polyoxometalate, Institute of Molecular and Crystal Engineering, College of Chemistry and Chemical Engineering, Henan University, Kaifeng, Henan, 475004, China.*

[b] *Fujian Provincial Key Laboratory of Polymer Materials, College of Chemistry and Chemical Engineering, Fujian Normal University, Fuzhou, Fujian, 350007, China.*

Experimental Section

Materials and Physical Measurements

All materials were commercially available and used as received. Infrared spectrum was recorded on a Bruker VERTEX-70 FT-IR spectrophotometer using a KBr pellet in the range of 400~4000 cm^{-1}. Elemental analyses were performed *via* Vario EL III Etro Elemental Analyzer. The solid-state circular dichroism (CD) spectrum was recorded on a MOS-450 Spectrometer with a KBr pellet. Thermogravimetric analysis (TGA) was performed in N_2 atmosphere with a heating rate of 10 °C/min^{-1} using TGA/SDTA851e. Powder X-ray diffraction (PXRD) pattern was recorded on a Philips X′PertPro instrument with Cu$K\alpha$ radiation (λ = 1.54056 Å) in the range 2 θ = 5–50 ° at room temperature. Magnetic measurements were carried out on a Quantum Design MPMS-XL SQUID magnetometer.

Crystallographical Section

X-ray single crystal data were collected at 296(2) K on a Bruker Apex-II CCD detector diffractometer with Mo$K\alpha$ radiation (λ = 0.71073 Å). Data reduction and absorption collection were made with empirical methods. The structures were solved by direct methods using SHELXS-97[1] and refined by full-matrix least-squares techniques using SHELXL-97.[2] Anisotropic displacement parameters were refined for most non-hydrogen atoms. And all hydrogen atoms bonded to C atoms were added in the riding model while the u_2-OH hydrogen atoms were located from the difference Fourier maps. As well, a D-camphoric acid ligand was disordered and C13, C14, C16 atoms in carbon ring and C17, C19 atoms in methyl were treated as two parts with occupancy of 50%, respectively. The crystal data and refinement details for compound **1** are listed in Table S1. The selected bond lengths and angles are listed in Table S2.

Table S1 Crystallographic data for compound **1**.

Compound	**1**
Empirical formula	$C_{50}H_{78}Ni_3O_{22}$
Formula weight	1207.25
Crystal system	Orthorhombic
Space group	$P2_12_12_1$
a (Å)	12.4370(6)
b (Å)	14.0606(7)
c (Å)	32.3952(16)
α (°)	90.00
β (°)	90.00
γ (°)	90.00
V (Å^3)	5665.0(5)
Z	4
T (K)	296(2)
D_c (g cm^{-3})	1.415
μ (mm^{-1})	1.063
Flack parameter	0.05(3)
F(000)	2552
θ limits (°)	1.58 to 25.00
Ref. collected	9927
Ref. unique	8442
R_{int}	0.0315
R index [$I>2\sigma(I)$]	$R_1 = 0.0618$, $wR_2 = 0.1562$
R(all data)	$R_1 = 0.0742$, $wR_2 = 0.1622$
GOOF	1.057
$\Delta\rho_{max}$/ $\Delta\rho_{min}$ (eÅ^{-3})	1.090/-1.346

$R = \sum(||F_o|-|F_c||)/\sum|F_o|$, $wR = \{\sum w[(F_o^2-F_c^2)^2]/\sum w[(F_o^2)^2]\}^{1/2}$, $w = 1/[\sigma^2(F_o^2)+(aP)^2+bP]$, $P = (F_o^2+2F_c^2)/3]$. **1**: $a = 0.0535$, $b = 24.5694$.

Table S2 Selected bond lengths [Å] and angles [°] for compound **1**.

Bond length (Å)			
Ni1–O8	1.993(5)	Ni2–O16	2.072(4)
Ni1–O6	2.016(5)	Ni2–O4	2.078(4)
Ni1–O10	2.029(4)	Ni2–O18	2.119(5)
Ni1–O12	2.038(4)	Ni3–O5	1.996(4)
Ni1–O22	2.078(4)	Ni3–O11	2.022(4)
Ni1–O21	2.083(5)	Ni3–O20	2.044(4)
Ni2–O7	1.990(5)	Ni3–O22	2.072(4)
Ni2–O9	2.056(4)	Ni3–O2	2.080(5)
Ni2–O21	2.080(5)	Ni3–O14	2.143(5)
Bond angles (°)			
O8–Ni1–O6	178.7(2)	O21–Ni2–O4	171.39(18)
O8–Ni1–O12	87.8(2)	O16–Ni2–O4	81.22(18)
O6–Ni1–O12	91.1(2)	O7–Ni2–O18	178.01(19)
O8–Ni1–O10	93.3(2)	O9–Ni2–O18	87.13(19)
O6–Ni1–O10	87.7(2)	O21–Ni2–O18	86.51(18)
O12–Ni1–O10	177.7(2)	O16–Ni2–O18	87.72(19)
O8–Ni1–O22	83.37(18)	O5–Ni3–O11	94.71(19)
O6–Ni1–O22	97.38(18)	O5–Ni3–O20	90.44(19)
O12–Ni1–O22	90.27(18)	O2–Ni3–O14	91.0(2)
O10–Ni1–O22	87.88(19)	O11–Ni3–O20	168.34(18)
O8–Ni1–O21	96.62(18)	O5–Ni3–O22	94.66(18)
O6–Ni1–O21	82.63(18)	O11–Ni3–O22	99.16(17)
O12–Ni1–O21	89.82(19)	O20–Ni3–O22	90.82(18)
O10–Ni1–O21	92.04(18)	O5–Ni3–O2	88.1(2)
O22–Ni1–O21	179.9(2)	O11–Ni3–O2	88.85(19)
O7–Ni2–O9	94.8(2)	O20–Ni3–O2	80.86(18)
O7–Ni2–O21	93.57(19)	O22–Ni3–O2	171.28(18)
O9–Ni2–O21	99.31(17)	O5–Ni3–O14	178.05(18)
O7–Ni2–O16	90.29(19)	O11–Ni3–O14	86.97(18)
O9–Ni2–O16	168.58(17)	O20–Ni3–O14	87.73(18)
O21–Ni2–O16	90.54(17)	O22–Ni3–O14	86.04(18)
O7–Ni2–O4	89.0(2)	Ni1–O21–Ni2	110.62(19)
O9–Ni2–O4	88.65(18)	Ni1–O22–Ni3	110.75(19)
O4–Ni2–O18	90.63(19)		

Table S3 BVS analyses of Ni and u_2-O atoms for **1**

Atoms	Ni1	Ni2	Ni3	u_2-O21	u_2-O22
BVS	2.125	1.983	2.021	0.630	0.641
Assignment	Ni^{2+}	Ni^{2+}	Ni^{2+}	OH^-	OH^-

The oxidation state of a particular atom can be taken as the nearest integer to the value. [3]

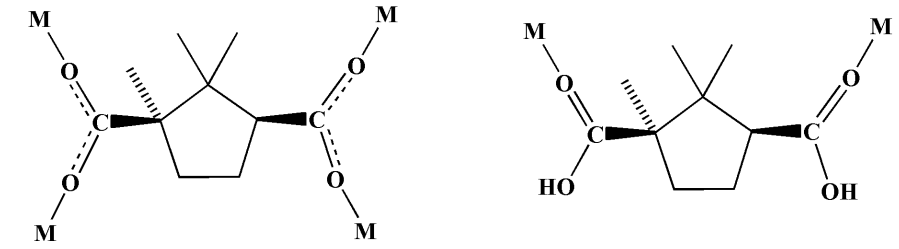

Scheme 1 Coordination modes of D-camphoric acid ligand in compound **1**.

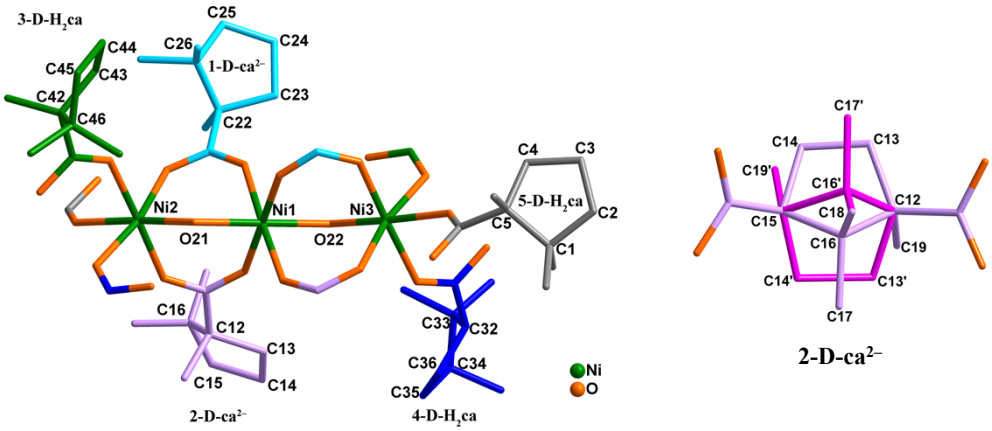

Fig. S1 Left: the asymmetric unit of compound **1**. Right: the 2-D-ca^{2-} is disordered and C13, C14, C16 in carbon ring as well as C17, C19 in methyl are treated as two parts with occupancy of 50% respectively in pink and rose red colors. H atoms are omitted.

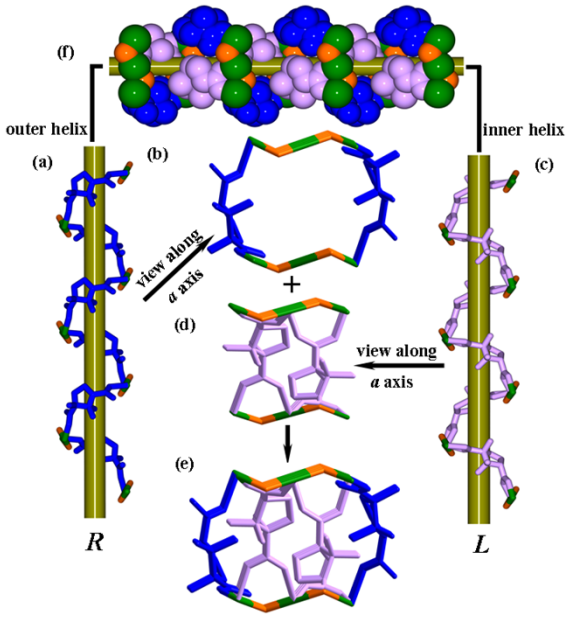

Fig. S2 The other type of nested coaxially helices of compound **1**. Color Scheme: Ni green; O orange. The D-camphoric acid ligands are in blue and pink colors for clarity. H atoms are omitted.

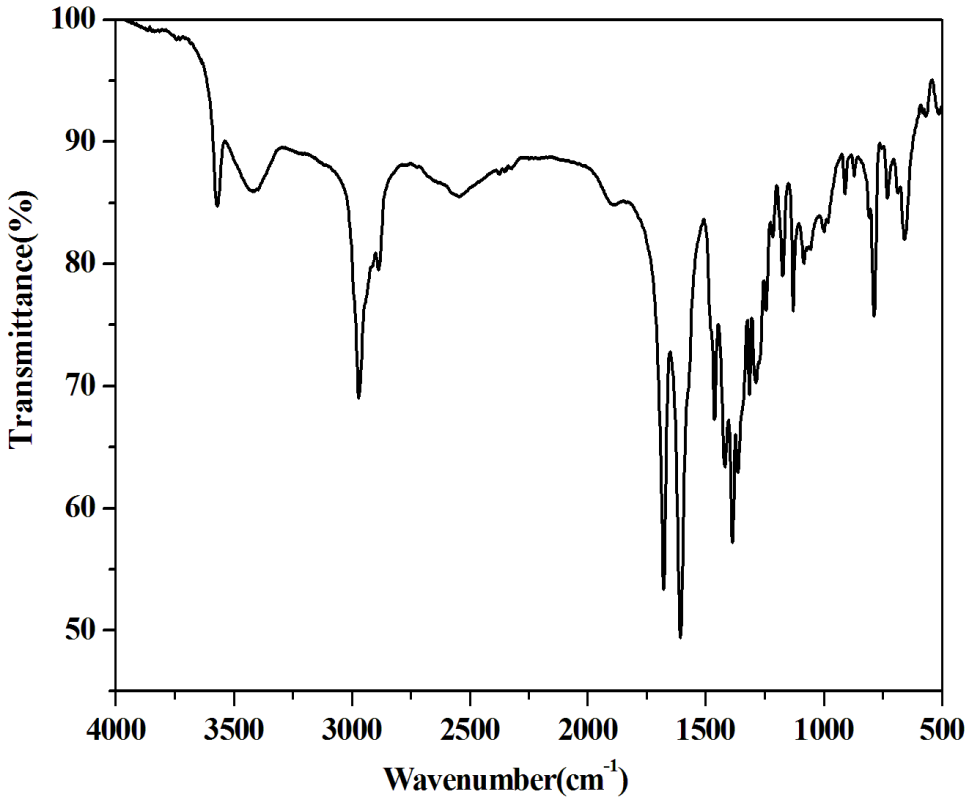

Fig. S3 IR spectrum for compound **1**.

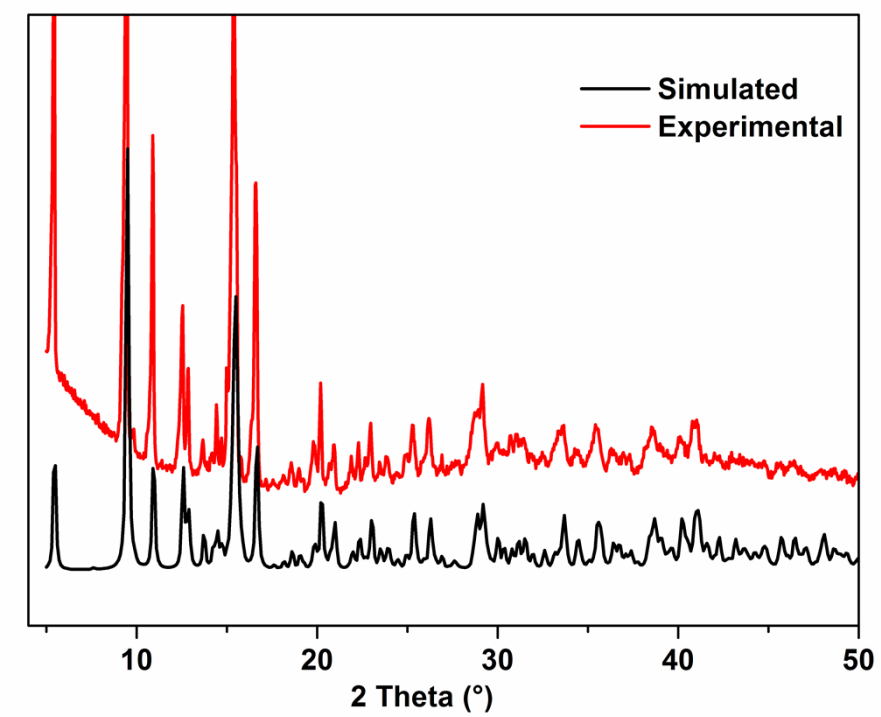

Fig. S4 PXRD curves for compound **1**.

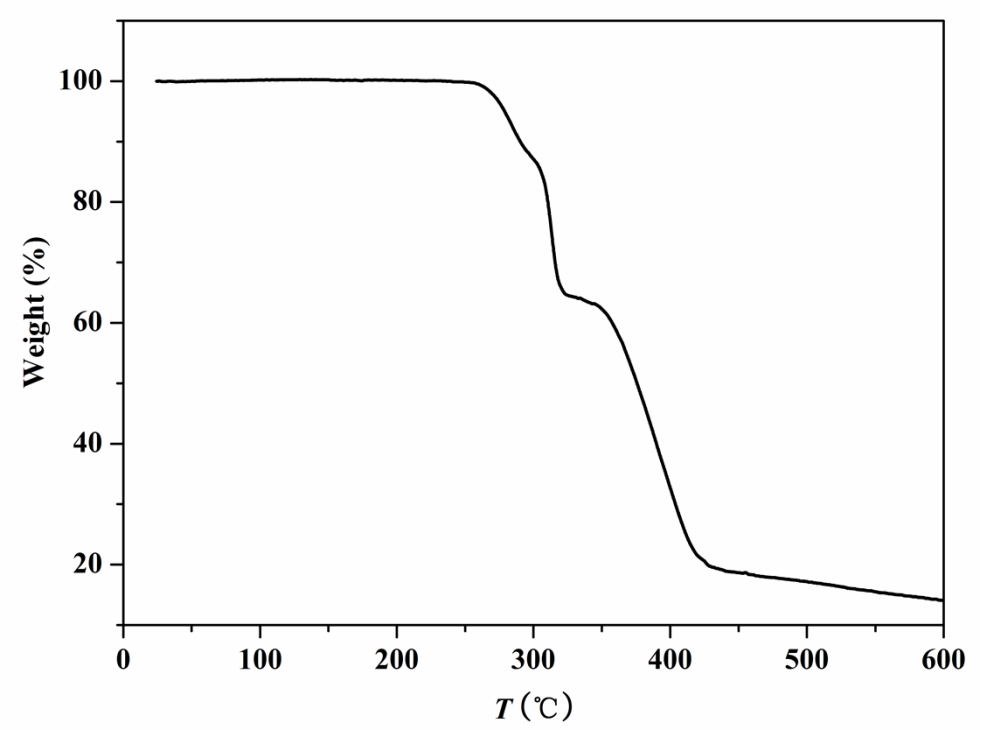

Fig. S5 TGA curve for compound **1**.

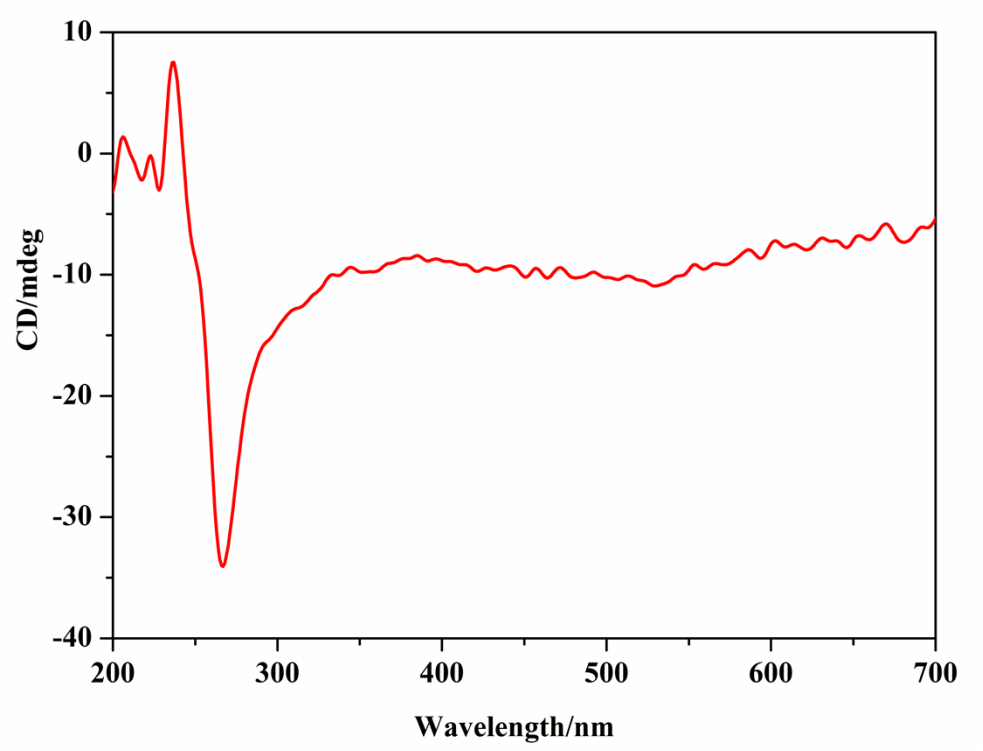

Fig. S6 CD spectrum of **1** in a KBr pellet.

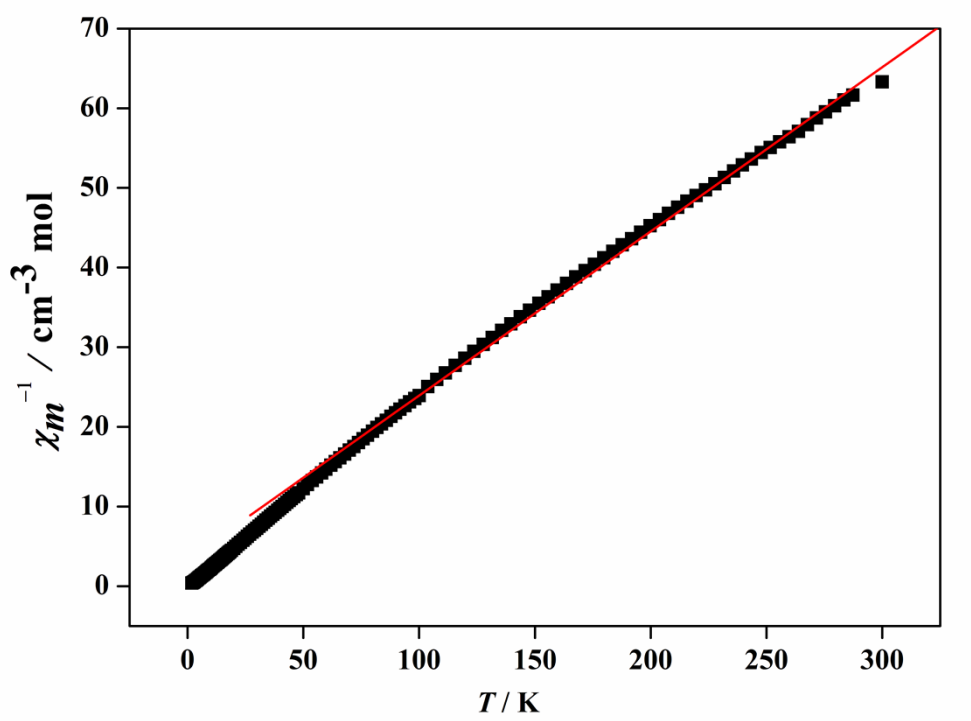

Fig. S7 The χ_m^{-1} *vs.* *T* plot of **1** in the range of 2–300 K at 1 KOe. The solid line is the best-fit above 80 K according to the Curie-Weiss law.

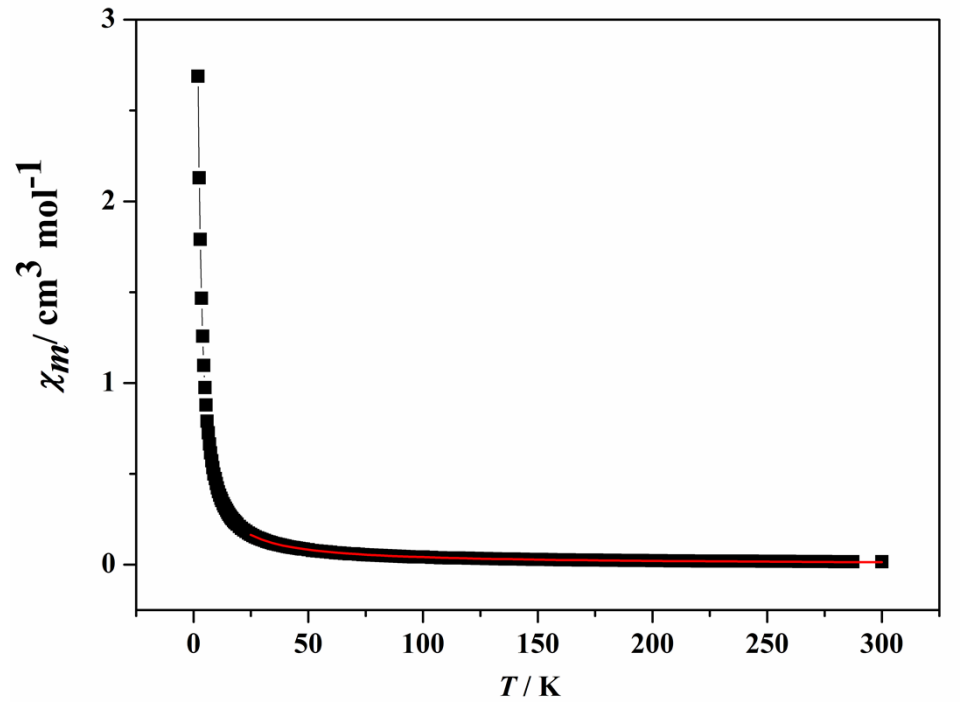

Fig. S8 The χ_m *vs.* *T* plot of **1** in the range 2-300 K at 1 kOe. The solid line is the best-fit above 25 K.

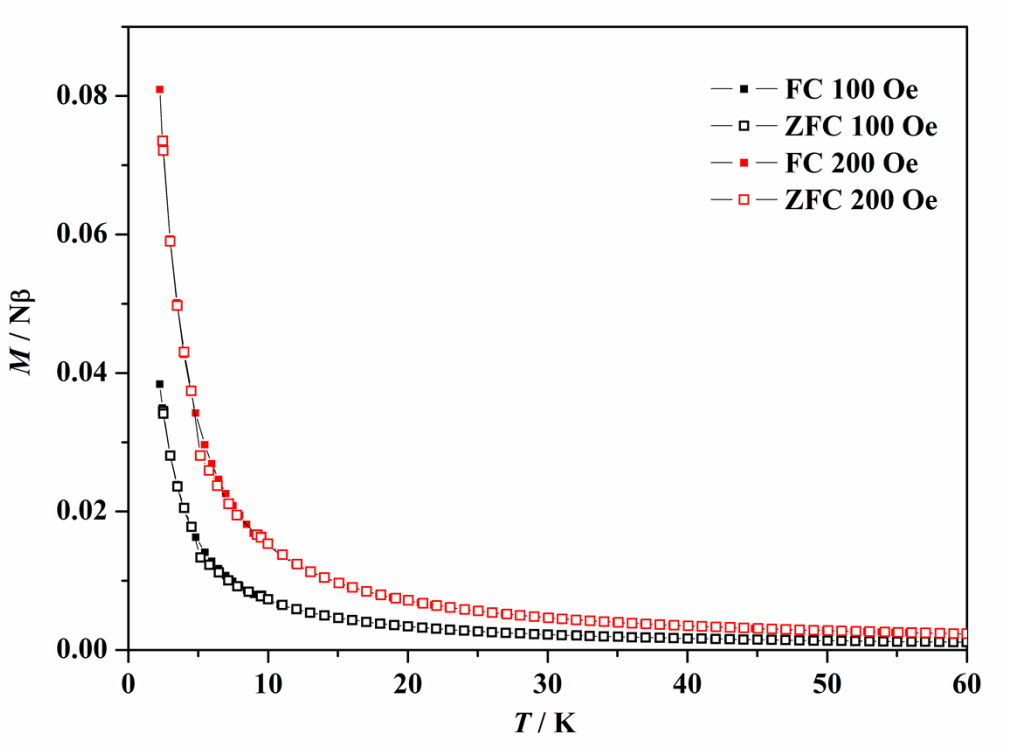

Fig. S9 FCM and ZFCM curves at 100 Oe and 200 Oe for **1**.

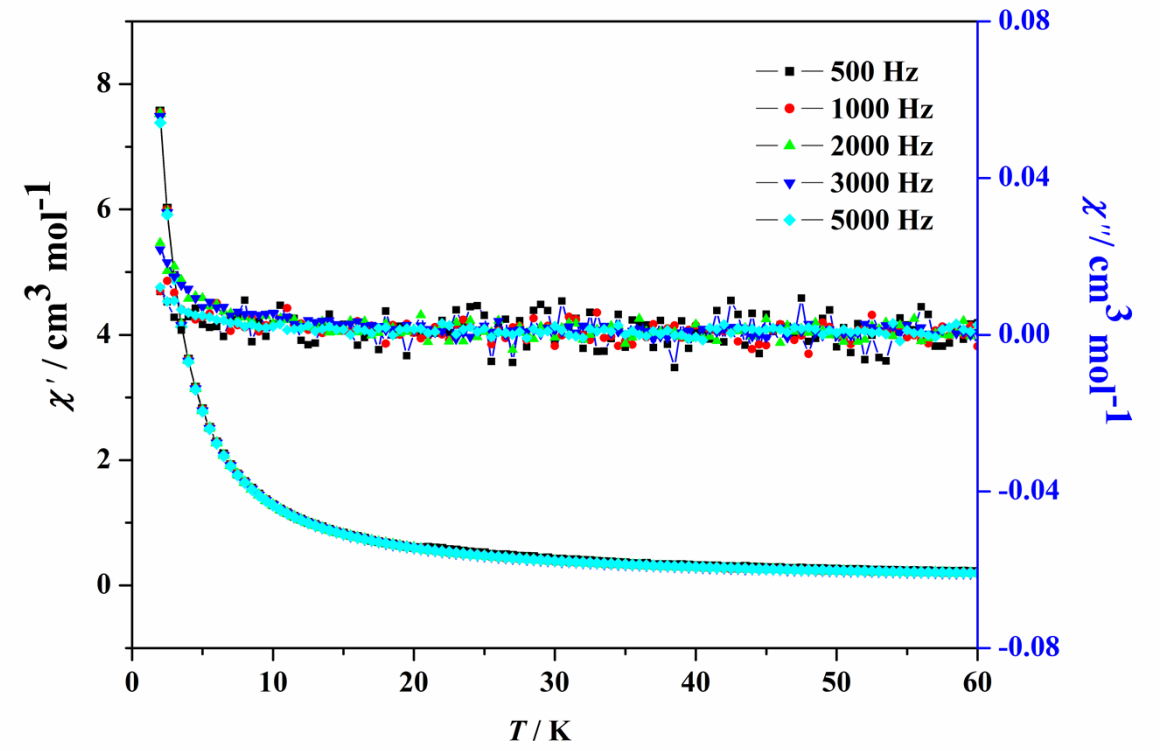

Fig. S10 Plots of the temperature dependence of the *ac* susceptibility χ' and χ'' obtained at 3 Oe field for **1**.

References

1 G. M. Sheldrick, SHELXS-97, *Program for X-ray Crystal Structure Solution*, University of Göttingen, Göttingen, Germany, 1997.

2 G. M. Sheldrick, SHELXL-97, *Program for X-ray Crystal Structure Refinement*, University of Göttingen, Göttingen, Germany, 1997.

3 P. van der Sluis and A. L. Spek, *Acta Cryst.*, 1990, **A46**, 194–201.